ELSEVIER

Surface Science 464 (2000) 48–56

surface science

www.elsevier.nl/locate/susc

Electronic structure of a Pt–Ge surface alloy

K. Fukutani [a,*], Y. Murata [b], J. Brillo [c], H. Kuhlenbek [c], H.-J. Freund [c], M. Taguchi [d]

[a] *Institute of Industrial Science, The University of Tokyo, Komaba, Meguro-ku, Tokyo 153-8505, Japan*
[b] *Physics Department, The University of Electro-Communications Chofugaoka, Chofu, Tokyo 182-8585, Japan*
[c] *Department of Chemical Physics, Fritz-Haber-Institut der Max--Planck-Gesellschaft, Faradayweg 4–6, D-14195 Berlin, Germany*
[d] *ULVAC-PHI Incorporated, 370 Enzo, Chigasaki 253-0084, Japan*

Received 8 May 2000; accepted for publication 11 July 2000

Abstract

The structural and electronic properties of a Pt(111)–Ge surface alloy are studied by scanning tunneling microscope and angle-resolved photoemission spectroscopy. The electronic band structure in the Γ–L direction was measured and compared with that of Pt(111). The crystal field parameters of $10Dq$ and ξ were evaluated to be 1.77 eV and 0.73 eV respectively. Alloying with Ge was found to reduce $10Dq$ and enhance ξ compared with pure Pt(111). © 2000 Elsevier Science B.V. All rights reserved.

Keywords: Alloys; Angle resolved photoemission; Germanium; Platinum; Scanning tunneling microscopy

1. Introduction

Investigation of binary alloys has long been a topic of great interest in both physics and chemistry. Alloy formation significantly alters the electronic structure of a material, serving as an important method to offer us new materials. For a detailed understanding of the alloy properties an accurate knowledge of the band structure is a strong requirement, and this has motivated experimental and theoretical studies such as photoemission spectroscopy and Korringa–Kohn–Rostoker coherent-potential approximation calculations. Of particular interest among a variety of systems is transition-metal and noble-metal-based alloys. Extensively studied systems are the Pd–Ag alloy [1,2] and related materials [3–5], where intermixing between the two electronic states and the degree of localized nature have been investigated. For a system of dilute alloys consisting of transition-metal host with non-transition metal impurity, the change of the spin paramagnetic susceptibility and the specific heat with increasing impurity concentration was examined for a variety of systems apparently indicating the d-band filling, which was also discussed theoretically in detail [6,7]. The advantage of the investigation of the dilute alloy is that the electronic structure of the host material is expected to be slightly perturbed and that the real effect on the electronic structure and the underlying mechanism of alloying can be clarified.

From a chemical point of view, a widely accepted idea is that d-electrons of a transition metal with a narrow band width play a crucial role in catalytic reactions. In heterogeneous catalysis, modification of a surface with other kinds of

* Corresponding author. Fax: +81-3-5452-6159.
E-mail address: fukutani@iis.u-tokyo.ac.jp (K. Fukutani)

PII: S0039-6028(00)00711-1

element, which includes the use of surfaces of bulk alloys and metal overlayer on a surface, is a frequently used technique to improve activity and selectivity in catalytic reactions [8–10]. Often encountered at a surface of bulk alloys is that the surface composition of an alloy is different from that of the bulk because of surface segregation. In recent years, surface alloys that are not stoichiometrically stable in the bulk phase have been formed on a pure metal surface and investigated experimentally as well as theoretically [11]. For Pt-based surface alloys a variety of elements, such as Sn [12,13], Cu [14], Ag [15], Co [16,17], Ge [18–20], Ce [21], Mn [22], Al [23], and Cr [24], are found to form surface alloys, and their properties from chemical features to electronic structures have been investigated.

The band structure of Pt was investigated in detail by angle-resolved photoemission spectroscopy (ARUPS) [25–29] and relativistic augmented-plane-wave calculations [30]. It was shown that the experimentally observed dispersion of the Pt d-bands is in good agreement with the calculation. From the spin-resolved measurements, the symmetry of the band was discussed [31,32]. Furthermore, surface resonance states are reported to be present at Pt(111) [33,34]. In our previous studies, we investigated adsorption of NO and CO molecules on the Pt(111)–Ge diluted surface alloy. We found that the binding energy of the molecules is substantially decreased and that the hollow-site adsorption taking place on the pure Pt(111) surface is dramatically suppressed on this surface [18,35,36], but that the occupied levels for adsorbed CO are almost the same as those on the pure Pt(111) surface [20]. We discussed the change of the chemical properties due to alloying in terms of the filling of the e_g band of the Pt substrate. The motivation behind the present study is to measure the band structure of the Pt(111)–Ge surface alloy, to elucidate the real effect of alloying, and to clarify the relation between the chemical properties and the electronic structure. In the present paper, we report scanning tunneling microscope (STM) observation and ARUPS measurements of the Pt(111)–Ge surface alloy, where we note appreciable perturbation of the host Pt by dilute alloy formation.

2. Experiment

The photoemission experiments were performed in an ultrahigh vacuum (UHV) chamber (base pressure: 1×10^{-10} mbar) equipped with low-energy electron diffraction (LEED) and a quadrupole mass spectrometer at the beamline TGM3 of the BESSY synchrotron radiation facility. The samples used were a pure Pt(111) surface and Pt(111) alloyed with Ge [Pt(111)–Ge]. The cleaning procedure of the sample has been described elsewhere [19,20]. The preparation of the Pt(111)–Ge surface alloy was performed by two monolayers of Ge deposition on Pt(111) followed by heating to 1300 K in the UHV chamber at the beamline. The alloy formation was confirmed by LEED[1] and the Ge 3d photoemission. Angle-resolved photoemission spectra were taken by a hemispherical electron energy analyzer at a pass energy of 5 eV. The overall energy resolution was about 0.2 eV. All spectra were measured for a sample at room temperature and a light incidence angle of 45° from the surface normal. Variation of the incident photon energy at the normal emission yields the dispersion of the energy bands in the Γ–L direction. After the photoemission experiments, the Pt(111)–Ge sample was transferred through atmosphere to a separate apparatus for STM (ULVAC-PHI) examination. Before STM measurements, the sample was heated at 1300 K, where the adsorbed gas due to exposure to air is removed and the Pt–Ge clean surface is recovered [18].

3. Results

Fig. 1a and b shows STM images of 10×10 nm^2 taken for Pt(111)–Ge at sample biases of -50 and -100 mV. In Fig. 1a, a 1×1 structure corresponding to the Pt–Pt interatomic distance is observed. On the other hand, bright spots arranged in 5×5 are observed in Fig. 1b. A naive idea is that these bright spots are attributed to Ge atoms

[1] We observed faint superspots corresponding to 5×5 at a primary energy E_p of lower than 50 eV. In Ref. [18], we reported a diffuse 1×1 for Pt(111)Ge probably because LEED was operated at $E_p>50$ eV.

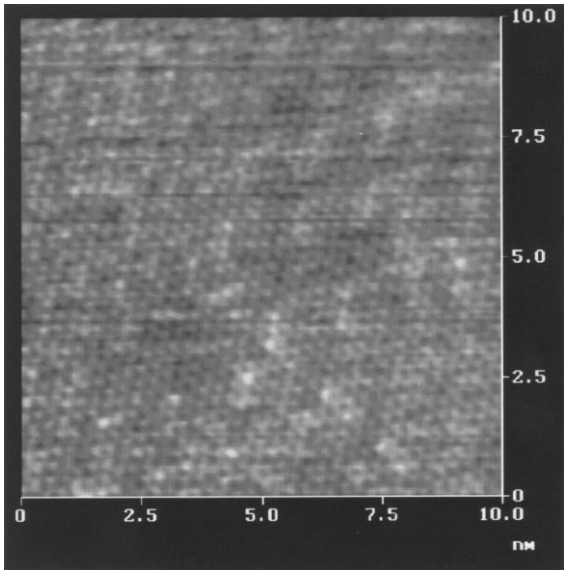

(a)

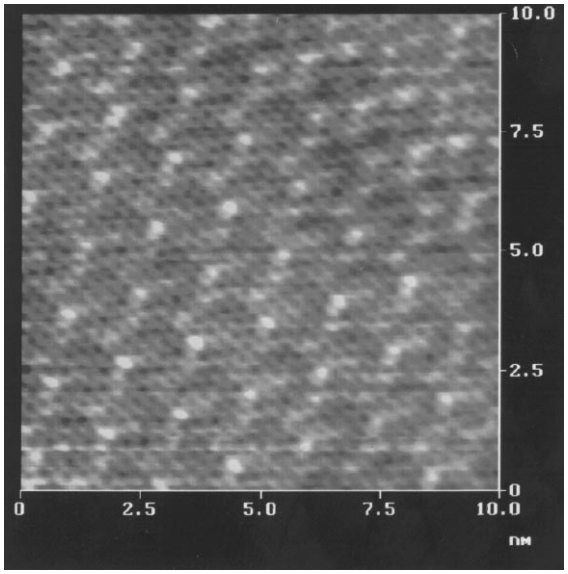

(b)

Fig. 1. STM images of the Pt(111)–Ge surface alloy for an area of $10 \times 10\ \mathrm{nm}^2$ at sample biases of (a) -50 mV and (b) -100 mV.

deposited on the Pt(111). Since the height difference between the bright atom and the others is small, the Ge atoms are considered to reside in the first layer of the Pt substrate forming a substitutional surface alloy. It is worth noting that these bright spots were also observed at positive biases of higher than 100 mV. In addition to these bright spots, one can see a slight contrast in the 5×5 unit that might be due to Ge atoms in the second layer. Assuming that Ge is arranged in 5×5 in the first layer, the Ge concentration in this surface alloy becomes 4%, which is roughly consistent with our previous Auger electron spectroscopy results [18] and the core-level spectra in the present work. Comparison of core-level emission intensities of Ge 3d and Pt 4f leads to a Ge concentration of 11% after correction of the difference in the photoionization cross-section [37]. According to the phase diagram of the Pt–Ge binary alloy [38], the most Pt-rich compound is reported to be Pt_3Ge. Therefore, this Ge-diluted alloy investigated in the present study is a surface alloy. It should be noted that we cannot exclude the possibility that the 5×5 structure is not a chemical contrast; it may be due to the charge density wave. In that case, the determination of the electronic dispersion along the surface parallel direction and the two-dimensional Fermi surface, and their temperature dependence would be an interesting topic for future study.

Figs. 2 and 3 show photoemission spectra at photon energies $h\nu$ from 10 to 48 eV for Pt(111) and Pt(111)–Ge respectively. Most of the features observed in Figs. 2 and 3 are direct transitions between the Pt bands, except for a feature observed at a binding energy E_B of 0.3 eV in all spectra and a feature at $E_B = 5.5$ eV with $h\nu = 22$ eV. The former peak has been reported to be assigned to the feature reflecting the total-density of states (TDOS) originating from the flat dispersion of the band 6 along the Q line in the reciprocal space, and the latter was assigned to a constant kinetic energy feature [26]. The overall spectral shape of Pt(111)–Ge is similar to that of Pt(111). A prominent difference is the peak position in the spectra. The spectra taken at $h\nu = 26$, 36 and 42 eV for the two surfaces are compared in Fig. 4a–c. Some of the peak positions for Pt(111)–Ge are obviously shifted compared with those of Pt(111). In Fig. 4a, the peaks corresponding to the direct transition are observed at $E_B = 1.17$ eV, 2.75 eV, and 4.05 eV for Pt(111), whereas they are observed at 1.27 eV, 2.76 eV, and 4.17 eV respectively for Pt(111)–Ge.

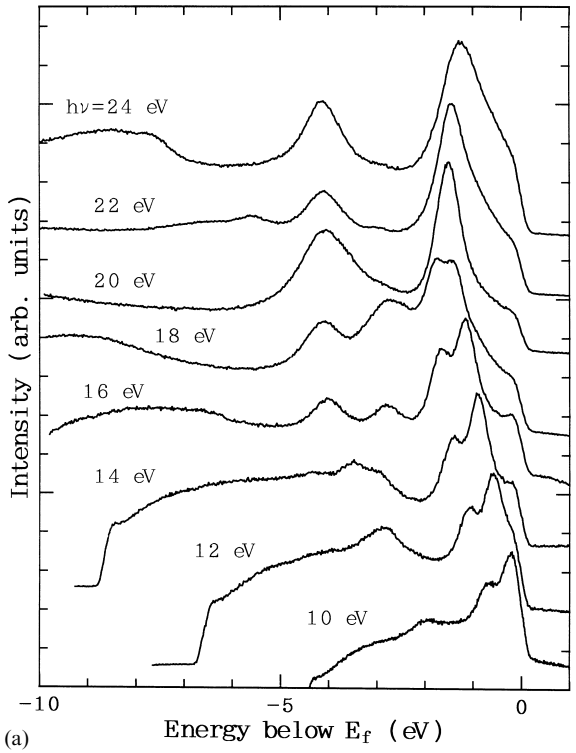

(a)

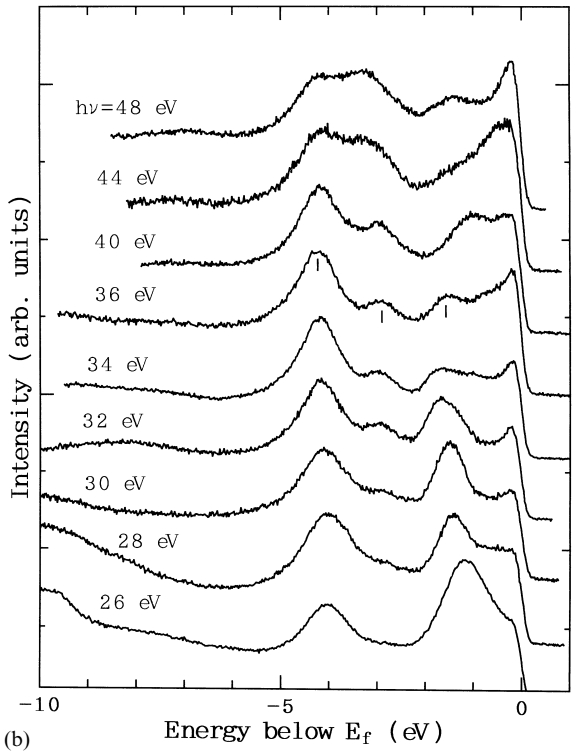

(b)

Fig. 2. ARUP spectra for Pt(111) in the normal emission at photon energies of 10–48 eV.

Similarly, peaks at $E_B = 1.58$ eV, 2.89 eV and 4.24 eV for Pt(111) are observed to be shifted to $E_B = 1.74$ eV, 2.75 eV, and 4.13 eV respectively for Pt(111)–Ge in Fig. 4b, and peaks at $E_B = 0.77$ eV, 2.89 eV, and 4.24 eV for Pt(111) are shifted to $E_B = 1.16$ eV, 2.75 eV and 3.99 eV respectively for Pt(111)–Ge in Fig. 4c. Note that the binding energy was carefully determined by fitting procedures, particularly for the weak peaks like that at about -2.75 eV in Fig. 4a. At first the background was fitted by a cubic polynomial as a function of the binding energy using the experimental data around the peak. After subtracting the background function, the peak was fitted to a Gaussian function, which gave us the peak position with an uncertainty of 0.01 eV. This fitting procedure was performed with different background subtractions, and the standard deviation for the peak position among these procedures turns out to be smaller than 0.03 eV. Care was also taken for the determination of the Fermi energy in each spectrum. Another difference observed in the spectra is the width of the peaks; the full width at half maximum (FWHM) of the peak at $E_B = 1.4$ eV in the spectra at $h\nu = 20$ eV is 0.59 eV for Pt(111) and 0.64 eV for Pt(111)–Ge. Also, the FWHM for the peak at $E_B = 4.2$ eV at $h\nu = 22$ eV is 0.73 eV for Pt(111) and 0.82 eV for Pt(111)–Ge respectively. The broadening of the peak can be attributed to the smearing effect due to dilute Ge.

The dispersion relations for Pt(111) and Pt(111)–Ge are shown in Figs. 5 and 6 respectively, together with the theoretical curves calculated by Andersen [30]. The FE-like band of $E(k) = \hbar^2 k^2/2m^* + V_0$ was assumed as the final state for the analysis, where m^* and V_0 are the effective mass and the band minimum respectively. Following the previous studies [26,30], we denote the five bands in Figs. 5 and 6 as bands 2–6. Although different values were used in the previous studies, $m^* = 1.27m_e$ and $V_0 = 0.4$ eV are chosen in the present study so that the bands 5 and 6 are well folded with respect to the Γ point. The three

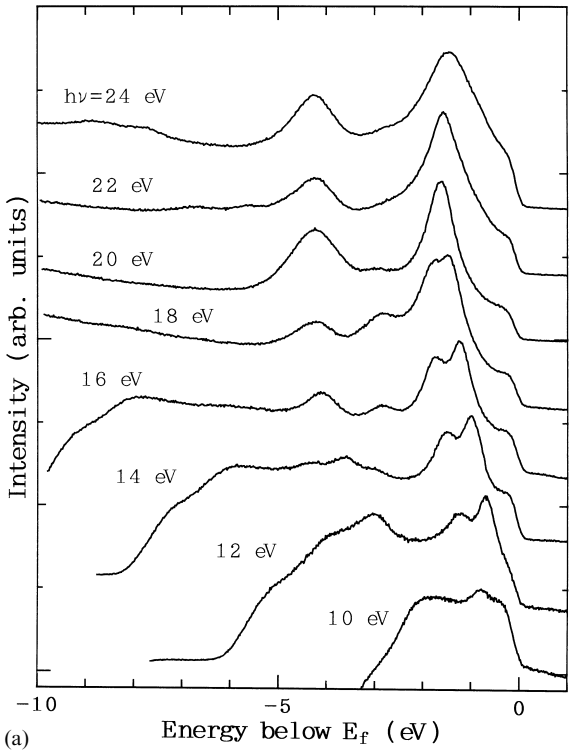

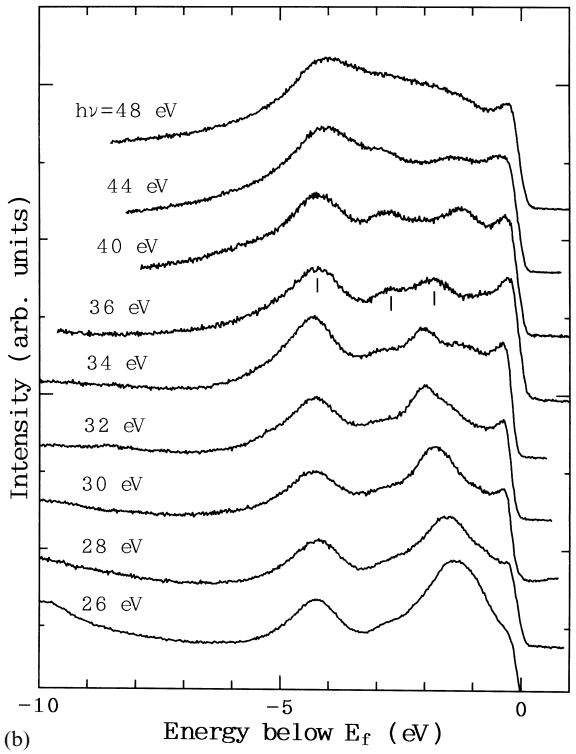

Fig. 3. ARUP spectra for Pt(111)–Ge in the normal emission at photon energies of 10–48 eV.

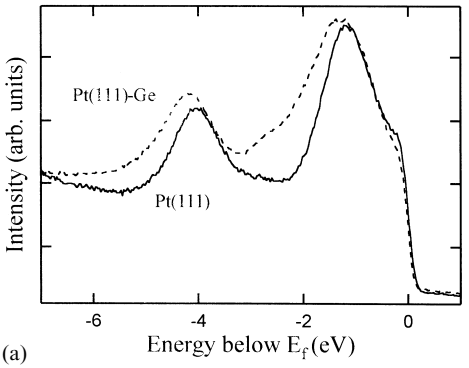

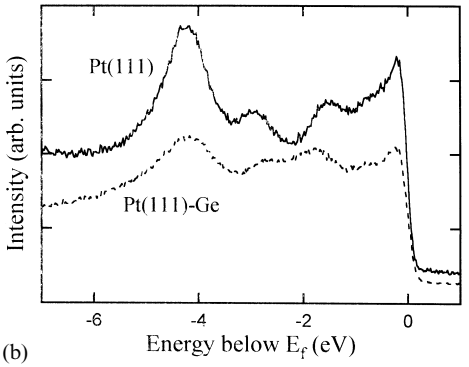

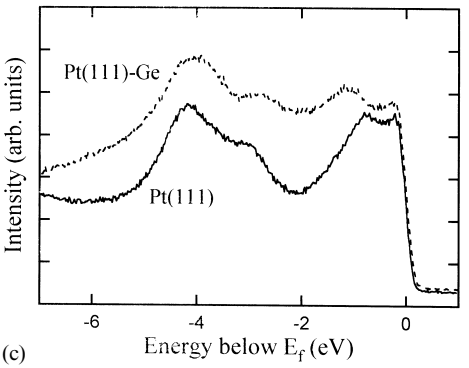

Fig. 4. ARUP spectra for Pt(111) (solid curve) and Pt(111)–Ge (broken curve) in the normal emission at photon energies of (a) 26 eV, (b) 36 eV, and (c) 42 eV.

spectra shown in Fig. 4 correspond to the spectra along the solid lines indicated by (a), (b) and (c) in Figs. 5 and 6 of the ***k***-vector versus energy

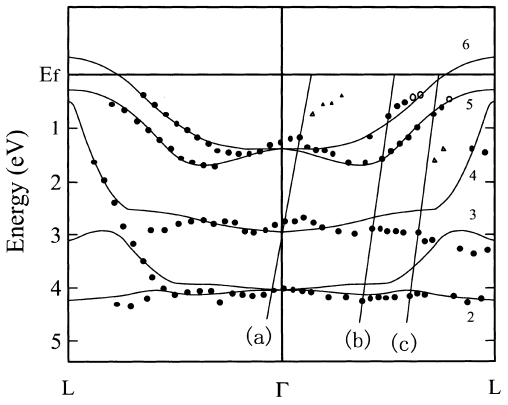

Fig. 5. Band structure of Pt(111) in Γ–L derived from the photoemission spectra (filled circles) assuming a free-electron (FE)-like final state with $m^* = 1.27m_e$ and $V_0 = 0.4$ eV. Triangles indicate weak peaks in the spectra. Ambiguous peaks near the Fermi level are shown by open circles. Theoretical curves by Andersen [30] are shown by solid lines. Solid lines (a)–(c) correspond to the spectra in Fig. 4a–c.

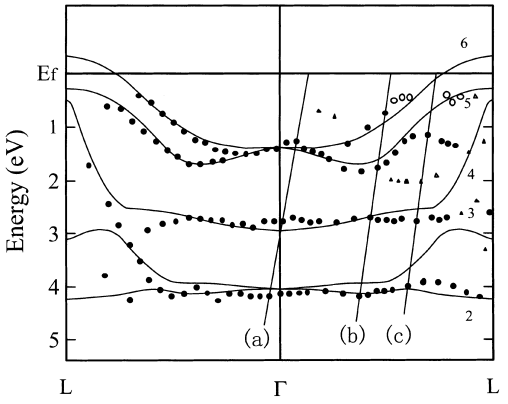

Fig. 6. Band structure of Pt(111)–Ge in Γ–L derived from the photoemission spectra (filled circles) assuming an FE-like final state with $m^* = 1.27m_e$ and $V_0 = 0.4$ eV. Triangles denote weak peaks in the spectra. Ambiguous peaks near the fermi level are shown by open circles. Theoretical curves by Andersen [30] are shown by solid lines. Solid lines (a)–(c) correspond to the spectra in Fig. 4a–c.

relation, and the three peaks in the spectra correspond to the bands 5, 4, and 2. The analysis of the peak corresponding to the bands 5 and 6 near the Fermi level contains large uncertainty compared with those well below the Fermi level because of the TDOS feature. However, comparing the spectrum at 40 eV with that at 36 eV, the peak at the Fermi level is obviously broadened, suggesting that an additional peak is present near the Fermi level. These peaks are indicated by open circles in Figs. 5 and 6. It should be noted that the 5×5 periodicity in Fig. 1 was observed in the surface parallel direction, not in the surface normal. Since no indication of superperiodicity is recognized in the dispersion relation of Fig. 6, the Ge atoms are considered to be randomly distributed in the surface normal direction. The same final state as that for Pt(111) was used for the analysis of the spectra for Pt(111)–Ge. If the lattice constant is changed by alloying with Ge, the final-state band should be so modified. However, the change of the lattice constant of this Pt(111)–Ge is expected to be -0.5%, in considering a Ge concentration of 4% and an atomic-radius difference of 12%. Hence, we consider that the final-state band is unchanged for Pt(111)–Ge. Although diluted Ge might cause modification to this final-state band, it is hard to interpret by this effect all the changes that appear in the spectra.

It is obvious that the dispersion relation of bands 5 and 6 for Pt(111)–Ge is not symmetric with respect to the Γ point. The band structure on the left-hand side of Fig. 6 is almost identical to that for Pt(111). Nevertheless, the dispersion on the right-hand side of Fig. 6 is definitely different. The separation of bands 5 and 6 is enhanced, and band 6 crossing the Fermi energy seems to be downward-shifted. Furthermore, the splitting of bands 2 and 4 at the Γ point is slightly increased from 1.27 to 1.40 eV.

We consider that this asymmetric feature of Fig. 6 is due to the difference of the probing depth. In the photon energy region used in this measurement, the mean free path of the photoelectron becomes shorter with increasing photon energy. Therefore, the measurements at higher photon energies as shown on the right-hand side of Fig. 6 reflect the band structure of the topmost layers. Although the thickness of the Pt(111)–Ge surface alloy is not known, it is inferred that the alloy layer extends to only a few layers.

4. Discussion

In order to derive the band structure from the photoemission data, an FE-like final state was

assumed, the parameters for which, m^* and V_0, cannot be unambiguously determined. Mills et al. [26] adopted $m^*=1.27m_e$ and $V_0=-1.2$ eV from an analogy with a similar final state for gold. On the other hand, Eyers et al. [31] used an FE-like final state with $m^*=1.1m_e$ and $V_0=-1.85$ eV, and a similar state of $m^*=1.1m_e$ and $V_0=-1.8$ eV was used by Leschik et al. [28]. In contrast to these previous studies, photoemission spectra were measured at higher photon energies in the present work, thus enabling us to make the bandmap of another Γ–L Brillouin zone and to examine the folded structure of the energy bands with respect to the zone boundary. With the effective mass fixed at $m^*=1.27m_e$, the experimental energy bands 2 and 3 were found by adjusting V_0 to fit well with the theoretical curves and to be symmetric with respect to the Γ point. With a smaller effective mass of $m^*=1.1m_e$, it was found that the experimental energy bands deviated from the theoretical curves to higher energy. It is noticed that a large dispersion observed for band 4 near the L point in the left-hand side of Fig. 5 (at low photon energies) is not clearly observed in the right-hand side of the figure.

Apart from the detailed structure, the crystal-field parameters can be discussed from the energy values of the bands at the Γ point. According to ligand-field theory [39,40], the Hamiltonian of a cubic system with crystal-field $10Dq$ and spin–orbit coupling ξ has three irreducible representations of $2\Gamma_8+\Gamma_7$, and the energy levels are described as

$$E(\Gamma_8)=6Dq+\sqrt{3/2}\xi\ cot\ \theta$$

$$E(\Gamma_7)=-4Dq+\xi$$

$$E(\Gamma_8)=-4Dq-\xi/2-\sqrt{3/2}\xi\ cot\ \theta,$$

where θ is defined as $tan\ 2\theta=-\sqrt{6}\xi/(10Dq+\xi/2)$. Since the band structure calculation without the spin–orbit coupling shows that the doubly degenerate Γ_{12} level lies at 1.5 eV and the triply degenerate $\Gamma_{25'}$ level lies at 3.6 eV below the Fermi level [41], the three energy levels correspond to the bands 5+6, 4 and 2+3 respectively. By solving the above equations for the two parameters with the energy levels of 1.26, 2.77, and 4.04 eV for Pt(111), $10Dq=1.87\pm0.10$ eV and $\xi=0.65\pm0.04$ eV were derived, which are roughly consistent with the previous study [26]. For the Pt(111)–Ge surface alloy, on the other hand, $10Dq$ and ξ are analyzed to be 1.77 ± 0.10 and 0.73 ± 0.03 eV respectively. Although the difference is small and not far beyond the experimental uncertainty, as displayed in the spectrum of Fig. 4a corresponding roughly to the Γ point, the band energies clearly shift toward each other. Therefore, one can conclude that the crystal field parameters are definitely modified by alloying: the value of $10Dq$ is reduced and the value of ξ is enhanced. Note that $10Dq$ and ξ mainly reflect the d electrons in the interatomic and near-core regions respectively, as discussed below. It is worth noting that alloy formation might lower the symmetry and lift the degeneracy of the bands.

We first discuss that the decrease of $10Dq$ can be interpreted in terms of the substitutional-alloy formation. On the basis of the linear-combination of atomic orbital (LCAO) scheme, the energies of the two d-bands at the Γ point are described by the on-site energy and the resonance integral of the d-orbitals [41,42]. One can find, from the *S*–*K* parameters [41], that the energy of $\Gamma_{25'}$ is mainly lowered by the first-neighbor interaction of the d_{xy} orbital in the [110] direction and equivalent interactions. On the other hand, the energy of Γ_{12} is mainly raised by the first-neighbor interaction of the $d_{x^2-y^2}$ orbital in the [110]. This indicates that the energy separation between $\Gamma_{25'}$ and Γ_{12} corresponding to $10Dq$ originates from the d–d interaction, which can be qualitatively understood by considering the symmetry of the two d-orbitals of d_{xy} and $d_{x^2-y^2}$. Since the formation of a substitutional alloy reduces the coordination number, we conclude that alloying decreases the interaction, leading to a reduction of the apparent crystal-field of $10Dq$.

In contrast to $10Dq$, the spin–orbit parameter ξ was increased from 0.65 eV to 0.73 eV by alloying. This increase is also displayed in the enhanced splitting between bands 5 and 6 in the Γ–L direction that has been confirmed to be due to the spin–orbit coupling experimentally and theoretically [43]; the maximum value of the splitting is increased from 0.54 eV for Pt(111) to 0.69 eV for

Pt(111)–Ge, which is consistent with the increase of ξ estimated at Γ. Since the spin–orbit coupling strength $\langle V_{so} \rangle$ is proportional to the gradient of the potential, wave functions near a nucleus contribute to $\langle V_{so} \rangle$ rather than those in the internuclear region. We consider that the enhancement of ξ is qualitatively consistent with the decrease of $10Dq$. The reduction of the d–d interaction described above causes the stronger localization of d wave functions leading to an increase of the wave-function amplitude near the nucleus.

Another prominent feature of the band structure for Pt(111)–Ge is the dispersion of band 6. As shown in the theoretical curve, band 6 of Pt(111) crosses the Fermi surface along the Γ–L, which was confirmed by previous de Haas–van Alphen measurements [44]. On the other hand, the energy of band 6 for Pt(111)–Ge seems to be lowered around the Fermi surface. We consider that this is due to the preferential filling of the e_g band, as discussed in our previous papers [18,19]. By constructing linear combinations of the p orbitals, $p_x + p_y$ and $p_x - p_y$, that are symmetric and asymmetric against the [110] respectively, one can understand that the Ge 4p orbital hybridizes effectively with the neighboring d_{xy} orbital in the [110] rather than $d_{x^2-y^2}$. According to the previous theory [7], the hybridization of the p orbital with the t_{2g} orbitals leads to a reduction of the DOS of t_{2g} in the low-energy part and causes an upward shift of the Fermi energy. As a result of this, the energy of the e_g band seems to be lowered compared with the t_{2g} band, which is in good agreement with the experimental results. This is qualitatively consistent with the downward shift of the Pt 4f core level by about 0.2 eV compared with that of pure Pt(111) [45].

The p–d hybridization is also consistent with the bias dependence of the STM; Ge atoms are observed as bright protrusions only at high bias voltages. The hybridization of the Ge 4p orbital and Pt 5d orbital leads to splitting of the p level into the bonding and antibonding levels. Taking into account the ionization potential of 7.88 eV for Ge, the bonding and antibonding levels are considered to be located below and above the Fermi level respectively, which is confirmed by an X-ray emission experiment [46], as well as by theoretical calculations [47], for a similar system of Si in Ni. Since the tunneling current of the STM is proportional to the local DOS, the bias dependence suggests higher DOS at the energies well below and above the Fermi level, which is qualitatively consistent with the picture of the p–d hybridization.

5. Conclusion

The geometric and electronic structure of a Pt(111)–Ge surface alloy was investigated by STM and ARUPS. Ge atoms were found to form a 5×5 structure, suggesting a Ge concentration of 4%. The band structure of this alloy in the Γ–L direction was found to be significantly modified by alloying. From crystal-field theory, the parameters $10Dq$ and ξ were evaluated to be 1.77 eV and 0.73 eV respectively. Alloying with Ge was found to reduce $10Dq$ and enhance ξ compared with pure Pt(111). The change of the electronic structure was discussed in terms of the reduction of the coordination number and the p–d hybridization.

Acknowledgements

This work was supported by Japanese–German Corporation Science Promotion Program of Japan Society for the Promotion of Science, and Bundesmisterium für Bildung und Forschung. This work was also supported by a Grant-in-Aid for Creative Basic Research and Scientific Research from the Ministry of Education, Science, Sports and Culture of Japan, Research Foundation For Materials Science and Nissan Science Foundation. One of the authors (KF) thanks a support by PRESTO, Research Development Corporation of Japan (JRDC).

References

[1] M. Pessa, H. Asonen, M. Lindroos, A.J. Pindor, B.L. Gyorffy, W. Temmerman, J. Phys. F: Met. Phys. 11 (1981) L33.

[2] D. van der Marel, G.A. Sawatzky, J.A. Julianus, J. Phys. F: 14 (1984) 281.
[3] T.-U. Nahm, R. Jung, J.-Y. Kim, W.-G. Park, S.-J. Oh, J.-H. Park, J.W. Allen, S.-M. Chung, Y.S. Lee, C.N. Whang, Phys. Rev. B 58 (1998) 9817.
[4] E. Arola, C.J. Barnes, R.S. Rao, A. Bansil, Phys. Rev. B 42 (1990) 8820.
[5] R.J. Cole, N.J. Brooks, P. Weightman, Phys. Rev. B 56 (1997) 12 178.
[6] T. Asada, K. Terakura, J. Phys. Soc. Jpn. 47 (1979) 1495.
[7] K. Terakura, J. Phys. F: 7 (1977) 1773.
[8] F.J.C.M. Toolenaar, F. Stoop, V. Ponec, J. Catal. 82 (1983) 1.
[9] V. Ponec, Adv. Catal. 32 (1983) 149.
[10] J.A. Rodriguez, Surf. Sci. Rep. 24 (1996) 223.
[11] A. Christensen, A.V. Ruban, P. Stoltze, K.W. Jacobsen, H.L. Skriver, J.K. Nørskov, F. Besenbacher, Phys. Rev. B 56 (1997) 5822.
[12] M.T. Paffett, S.C. Gebhard, R.G. Windham, B.E. Koel, J. Phys. Chem. 94 (1990) 6831.
[13] C. Xu, B.E. Koel, Surf. Sci. 327 (1995) 38.
[14] U. Schneider, G.R. Castro, K. Wandelt, Surf. Sci. 287–288 (1993) 146.
[15] H. Röder, R. Schuster, H. Brune, K. Kern, Phys. Rev. Lett. 71 (1993) 2086.
[16] M. Galeotti, A. Atrei, U. Bardi, B. Cortigiani, G. Rovida, M. Torrini, Surf. Sci. 297 (1993) 202.
[17] J.S. Tsay, C.S. Shern, Surf. Sci. 396 (1998) 313.
[18] K. Fukutani, T.T. Magkoev, Y. Murata, K. Terakura, Surf. Sci. 363 (1996) 185.
[19] K. Fukutani, T.T. Magkoev, Y. Murata, K. Terakura, in: Elementary Processes in Excitations and Reactions on Solid Surfaces, Springer Series in Solid-State Sciences, vol. 121, Springer, Berlin, 1996, p. 217.
[20] K. Fukutani, T.T. Magkoev, Y. Murata, M. Matsumoto, T. Kawauchi, T. Magome, Y. Tezuka, S. Shin, J. Electron Spectrosc. Relat. Phenom. 88–91 (1998) 597.
[21] C.J. Baddeley, A.W. Stephenson, C. Hardacre, M. Tikhov, R.M. Lambert, Phys. Rev. B 56 (1997) 12 589.
[22] S. Gallego, C. Ocal, M.C. Munoz, F. Soria, Phys. Rev. B 56 (1997) 12 139.
[23] K. Wilson, J. Brake, A.F. Lee, R.M. Lambert, Surf. Sci. 387 (1997) 257.
[24] L. Zhang, J. van Ek, U. Diebold, Phys. Rev. B 57 (1998) 4285.
[25] N.V. Smith, Phys. Rev. B 9 (1974) 1365.
[26] K.A. Mills, R.F. Davis, S.D. Kevan, G. Thornton, D.A. Shirley, Phys. Rev. B 22 (1980) 581.
[27] G. Thornton, R.F. Davis, K.A. Mills, D.A. Shirley, Solid State Commun. 34 (1980) 87.
[28] G. Leschik, R. Courths, H. Wern, S. Hüfner, H. Eckardt, J. Noffke, Solid State Commun. 52 (1984) 221.
[29] V.M. Tapilin, D.Y. Zemlyanov, M.Y. Smirnov, V.V. Gorodetskii, Surf. Sci. 310 (1994) 155.
[30] O.K. Andersen, Phys. Rev. B 2 (1970) 883.
[31] A. Eyers, F. Schäfers, G. Schönhense, U. Heinzmann, H.P. Oepen, K. Hünlich, J. Kirschner, G. Borstel, Phys. Rev. Lett. 52 (1984) 1559.
[32] H.P. Oepen, K. Hünlich, J. Kirschner, A. Eyers, F. Schäfers, G. Schönhense, U. Heinzmann, Phys. Rev. B 31 (1985) 6846.
[33] W. Di, K.E. Smith, S.D. Kevan, Phys. Rev. B 43 (1991) 12 062.
[34] W. Di, K.E. Smith, S.D. Kevan, Phys. Rev. B 45 (1992) 3652.
[35] M. Matsumoto, N. Tatsumi, K. Fukutani, T. Okano, T. Yamada, K. Miyake, K. Hata, H. Shigekawa, J. Vac. Sci. Technol. A: 17 (1999) 1577.
[36] M. Matsumoto, K. Fukutani, T. Okano, K. Miyake, H. Shigekawa, H. Kato, H. Okuyama, M. Kawai, Surf. Sci. 454–456 (2000) 101.
[37] J.J. Yeh, I. Lindau, At. Data Nucl. Data Tables 32 (1985) 1.
[38] T.B. Massalski, H. Okamoto, P.R. Subramanian, L. Kacprzak (Eds.), Binary Alloy Phase Diagrams, second edition, ASM, 1990.
[39] C.J. Ballhausen, Introduction to Ligand Field Theory, McGraw-Hill, New York, 1962.
[40] P.S. Wehner, R.S. Williams, S.D. Kevan, D. Denley, D.A. Shirley, Phys. Rev. B 19 (1979) 6164.
[41] D.A. Papaconstantopoulos, in: Handbook of the Band Structure of Elemental Solids, Plenum, New York, 1986, p. 198.
[42] J.C. Slater, G.F. Koster, Phys. Rev. 94 (1954) 1498.
[43] L.F. Mattheiss, R.E. Dietz, Phys. Rev. B 22 (1980) 1663.
[44] D.H. Dye, J.B. Ketterson, G.W. Crabtree, J. Low Temp. Phys. 30 (1978) 813.
[45] K. Fukutani, T.T. Magkoev, Y. Murata, Y. Tezuka, S. Shin unpublished results.
[46] K. Tanaka, M. Matsumoto, S. Maruno, A. Hiraki, Appl. Phys. Lett. 27 (1975) 529.
[47] K. Terakura, J. Phys. Soc. Jpn. 40 (1976) 450.